CHAPTER 4: ANALYSIS AND MODELLING

TABLE OF CONTENTS

		Page
4	**ANALYSIS AND MODELLING**	**4-1**
4.1	**INTRODUCTION**	**4-1**
4.2	**DISCUSSION OF LABORATORY RESULTS**	**4-1**
4.2.1	Deflection	4-1
4.2.2	Horizontal crack displacement	4-2
4.2.3	Load transfer efficiency	4-3
4.2.4	Relative movement	4-4
4.2.5	Aggregate interlock joint/crack shear stiffness	4-6
4.3	**ANALYSIS OF FIELD DATA**	**4-9**
4.3.1	Relative movement analysis	4-10
4.3.2	Aggregate interlock joint/crack shear stiffness	4-13
4.3.3	South African mechanistic concrete pavement design software	4-14
4.4	**CONCLUSIONS**	**4-14**

LIST OF TABLES

Table 4.1: Comparison between South African and USA aggregate properties 4-3
Table 4.2: Input values for calculating shear stiffness (*AGG*) of crack faces 4-6
Table 4.3: Average increase in *AGG* due to dynamic loading 4-9
Table 4.4: Summary of FWD test results for all road sections 4-9
Table 4.5: Input values for calculating shear stiffness (*AGG*) of crack faces 4-13

LIST OF FIGURES

Figure 4.1: Relative movement at joint – 20 kN versus 40 kN static loading for 19 mm and 37,5 mm coarse aggregates 4-5
Figure 4.2: Joint shear stiffness versus crack width for static loading LTE results of aggregate interlock experiments 4-7
Figure 4.3: Joint shear stiffness versus crack width for static loading LTE results of the plastic joint 4-8
Figure 4.4: Simulated deflection across joint – Road Section 1 4-11
Figure 4.5: Simulated deflection across joint – Road Section 2 4-11
Figure 4.6: Simulated deflection across joint – Road Section 3 4-12
Figure 4.7: Simulated deflection across joint – Road Section 4 4-12

Figure 4.8: LTE versus joint stiffness calculated for field data 4-14

LIST OF SYMBOLS / ABBREVIATIONS

C	Continuous
DC	Discontinuous
LTE	Load transfer efficiency
RM	Relative movement
VST	Volumetric surface texture
VSTR	Volumetric surface texture ratio

4 ANALYSIS AND MODELLING

4.1 INTRODUCTION

Following on Chapter 3 in which the laboratory and the field data were discussed in detail, this chapter further summarises the results and points the way to specific applications of the results from this research project. The application of the aggregate interlock equation developed as the primary objective of this thesis is described in Chapter 5.

4.2 DISCUSSION OF LABORATORY RESULTS

4.2.1 Deflection

An increase in crack width caused an increase in deflection. For Experiments 1 and 2, the repeated dynamic loads caused the slab to stay in a deflected state with deflections higher than under static loading at small crack widths. The dynamic loading line crossed the static loading line at a crack width of between 1,0 and 1,1 mm. At this crack width the two slabs started to react independent of each other, resulting in higher deflections under static loading than dynamic loading (see also Figures 3.5 and 3.13). The larger 37,5 mm aggregate had lower deflections than the smaller 19 mm aggregate at the same crack widths during dynamic and static loading at crack widths larger than 1,1 mm. This confirmed the greater resistance to deflection movement of the larger aggregate.

The deflections measured during Experiments 3 and 4 were lower than for Experiments 1 and 2. Furthermore, contrary to the situation where the dynamic and static loading lines crossed at a crack width of between 1,0 and 1,1 mm during Experiments 1 and 2, the dynamic loading line was constantly higher than the static loading line during Experiments 3 and 4.

The deflection results of Experiments 1 and 2 (see Figures 3.5 and 3.13) on the C rubber subbase were approximately 3 times higher than the comparative results of Experiments 3 and 4 (see Figures 3.17 and 3.25). This difference in deflection results was primarily due to the C rubber subbase that allowed larger shear forces to be transferred from the leave slab to the approach slab than the DC rubber subbase.

The results from Experiments 3 and 4 corresponded better with published results (Jensen, 2001). Jensen (2001) compared the response of 25 mm limestone, 25 mm glacial gravel, and a 50 mm glacial gravel blend under 40 kN static loading. The deflections obtained by Jensen (2001), especially for 25 mm limestone, corresponded well with the 40 kN results obtained for 19 mm dolomite in Experiment 3 (see Figure 3.22).

It is the opinion of the author that the response of the plastic joint was that measured up to a crack width of 1,5 mm, and that specifically the results under dynamic loading thereafter were influenced by the subbase stiffness. This would imply that the smoother the texture of the crack face, the sooner the system would rely on the support of the subbase to transfer stresses and strains from one slab to another. This study has already indicated three such transition zones, namely: 1,5 mm for the smooth joint, 2,5 mm for the 19 mm aggregate interlock joint, and between 3,5 mm and 4,0 mm for the 37,5 mm aggregate interlock joint.

EverFE (Davids et al., 1998a) was used to perform theoretical analyses. Up to a crack width of 0,5 mm EverFE predicted initial deflection values similar to what was measured in the laboratory. However, at crack widths larger than 0,5 mm there was a smaller increase in deflection with increasing crack width. The results seemed to reach an asymptote and were eventually far less than those measured during execution of Experiments 1 and 2, but slightly higher than the results of Experiments 3 and 4. The main reason for the difference in results could be attributed to the foundation model used in the EverFE software, as described in paragraph 3.2.1 in Chapter 3.

4.2.2 Horizontal crack displacement

The main function of the clip gauges at the top and bottom of both sides of the crack was to control the crack width during opening and closing of the two parts of the slab for deflection testing at different crack widths. Analysis of the data rendered interesting information regarding the opening-closing movements across the crack.

The magnitude of the horizontal crack displacement measurements were both influenced by the methods applied to open and close the slab, as well as by the type of subbase beneath the slab. The C rubber subbase allowed far greater movement than the DC rubber subbase.

At small crack widths (< 0,5 mm) the bottom crack displacement measurements tended to be higher than the top crack displacement measurements (Figures 3.18, 3.19, 3.44 and 3.45). In other words, the slab tended to bend through with the top of the crack closing, and the bottom of the crack opening during loading at narrow crack widths.

At crack widths greater than 0,5 mm this was reversed with the top crack displacement becoming larger than the bottom crack displacement, indicating that the crack was being pushed open during loading. The movement at the top of the crack under dynamic loading was approximately twice as much as the movement under static loading, which could be attributed to the effects of momentum. This demonstrated why large crack widths are so detrimental to pavement performance, as the opening up of the crack at the top during loading, makes it easier for debris and loose particles to be driven into the cracks, which in turn cause spalling of the concrete at the crack face.

4.2.3 Load transfer efficiency

The deflection LTE obtained for both dynamic and static loading for the first four experiments at different crack widths was presented graphically on Figures 3.7, 3.14, 3.20, and 3.28.

Firstly, the deflection LTE was greater during dynamic than static loading in all instances. Larger maximum sized aggregates had greater deflection load transfer efficiencies than smaller maximum sized aggregates. For the same maximum aggregate size concrete mixes, the LTE was larger where there was a C subbase support (rubber not cut through) than where there was a crack simulated into the subbase (top rubber layer cut through). The LTE on the C subbase was on average 105% that of the DC subbase, for both dynamic and static loading.

Due to the effect of greater momentum forces acting across the crack, the LTE under 40 kN static loading was slightly higher than under 20 kN static loading.

Demonstration of the contribution of the high quality crushed stone used in manufacturing concrete pavements in Southern Africa is of great importance. The formulae used in the software package, EverFE, are mostly based on experimental results obtained from tests conducted on concrete pavements constructed with the lesser quality aggregates found in the USA. To quantify this statement, the relevant properties of the granite and dolomite used for this research study were compared with those of the limestone and glacial gravel used by Jensen (2001) (see Table 4.1).

The physical properties of the South African aggregates were obtained from the suppliers of the materials, and the properties of the USA aggregates not reported by Jensen (2001) were obtained from the Nordberg Process Machinery Reference Manual (1983).

Table 4.1: Comparison between South African and USA aggregate properties

Aggregate type	Description of test				
	Aggregate crushing value (%)	Relative density (kg/m^3)	Water absorption (%)	Los Angeles abrasion value (%)	Stiffness modulus (GPa)
South Africa					
Granite (19 mm)	25	2,65	0,33	33	27,0
Granite (37,5 mm)	27	2,65	0,33	33	29,0
Dolomite (19 mm)	15	2,86	0,2	21	42,0
Dolomite (37,5 mm)	15	2,86	0,2	21	48,0
USA					
Limestone (25 mm)	18	2,61	0,61	34	22,0
Glacial gravel (50 mm)	30	2,58	-	22	24,0

The crushing value of the limestone was similar to that of the dolomite, and that of the glacial gravel slightly higher than the granite aggregate. The relative densities of the USA aggregates were slightly less than the South African granite, with the water absorption of the limestone twice as high as that of the granite aggregate. The Los Angeles abrasion value of the South African granite aggregate compared well with that of the USA limestone, and the South African dolomite and USA glacial gravel had similar results. The important difference in physical properties lay in the lower stiffness moduli of the USA aggregates, where both the limestone and glacial gravel had lower stiffnesses than the South African granite. As mentioned before, the granite was chosen as representative of the weaker of the concrete construction aggregates crushed in South Africa, and that the stiffness of the aggregate largely contributes to the stiffness of the concrete. This would imply that the concrete constructed with low stiffness aggregates would be less resistant to cracking and abrasion than the concrete constructed with stronger aggregates.

When comparing the results published by Jensen (2001) during a similar study using typical aggregates found in the USA with the results obtained in this study, it was obvious that even though the deflections were similar, the LTE achieved using South African crushed stone were significantly higher. The 50 mm glacial gravel blend, the largest aggregate size used by Jensen (2001), rendered load transfer efficiencies of less than 80% at a crack width of 2,5 mm. On the other hand for the comparatively small 19 mm dolomite aggregate used in this study a LTE of 84% was calculated for the same crack width.

The fact that little abrasion occurred at the crack face during testing inside the laboratory was confirmed by Will Hansen (2003) through follow-up testing conducted on the experimental slabs used in the study of which preliminary results were published during 2001 (Jensen, 2001). This was despite the fact that they used softer aggregates with lower relative densities and stiffness moduli, and also had lower concrete strengths than what was achieved in this study (see Table 4.1).

Another tool that was used to quantify that the South African crushed aggregates are more angular and have a greater aggregate interlock potential than the USA aggregates, was through VST testing (Vandenbossche, 1999) as described in Appendix F. The VSTR results obtained for the 19 mm and 37,5 mm coarse aggregate concrete were 37% and 44%, respectively, higher then the USA results (see Photo G.25). VST has however not been included in the modelling effort, as no South African field data was available to calibrate the laboratory results. Obtaining such field data from the road sections investigated was also not considered viable, as it would have been a too costly exercise.

4.2.4 Relative movement

Some researchers are of the opinion that the generally accepted method of determining the efficiency of a joint in terms of deflection LTE is not necessarily the correct method, as it gives results based on the efficiency of the whole system. In other words, measuring efficiency in terms of LTE not only takes

into account the deflection of the concrete slab, but also the deflection of the subbase and subgrade. On the other hand, it was stated that when analysing the RM measured on top of the concrete, the deflection of the concrete is isolated (Strauss, 2001).

This further led to the assumption that the RM data of similar coarse aggregate concrete mixes should have the same RM results, irrespective of the type of subbase support. The RM measured for both aggregate types at different crack widths for dynamic and static loading, respectively, were approximately the same. Logistic regression equations were therefore fitted to the data in terms of relative movement (y) versus crack width (x) for both 19 mm and 37,5 mm maximum sized aggregate (Equations (3.2) to (3.5)).

These logistic equations were developed from data where a single 20 kN truck wheel load crossed the joint/crack, and it was therefore still necessary to determine the effect of a 40 kN dual wheel load crossing the joint/crack. Equations (3.3) and (3.5) were plotted against the relative movement data obtained during application of the 40 kN static loads at one side of the crack during Experiments 3 and 4 (see Figure 4.1). From this figure it is clear that the curves fitted to the data are basically the same. The 40 kN data for the 19 mm maximum sized aggregate being slightly higher than the plot of Equation (3.3), and the 40 kN data for the 37,5 mm maximum sized aggregate slightly lower than the plot of Equation (3.5). It can therefore be assumed that the relative movement induced at a joint/crack by an 80 kN dual wheel truck axle crossing the joint will be that caused by each 20 kN wheel crossing the joint/crack.

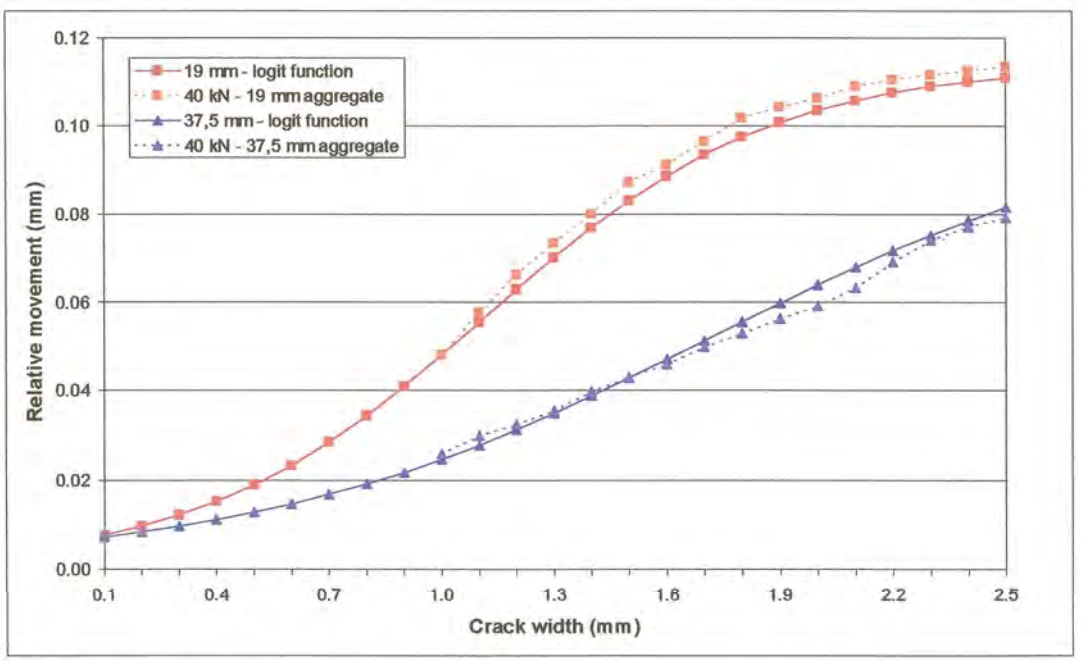

Figure 4.1: Relative movement at joint – 20 kN versus 40 kN static loading for 19 mm and 37,5 mm coarse aggregates

Although the RM results for the same coarse aggregate size mixes were similar, and it was possible to calculate the average RM from different experiments, this approach is not logical. There are three components involved during load transfer at a joint/crack, namely: the portion carried by the slab, the portion carried by the subbase/subgrade, and the portion carried by the load transfer mechanism. These components have to be in equilibrium, and during the measurement of LTE, if one carries more of the imposed load, the others will carry less.

The real contribution from the RM data was the development of a single equation that has already been incorporated in the source code of the CncRisk software, as discussed below.

4.2.5 Aggregate interlock joint/crack shear stiffness

The relationship between deflection LTE and the dimensionless joint stiffness (*AGG/kl*) developed by Ioannides and Korovesis (1990) was used to calculate the shear stiffness per unit length (*AGG*) of the crack faces of the experimental slabs. The LTE calculated from the laboratory deflections, together with Equation B.44 (Appendix B) was used. The values used in the calculation of the shear stiffness are summarised in Table 4.2.

Table 4.2: Input values for calculating shear stiffness (*AGG*) of crack faces

Description	Granite		Dolomite		Plastic joint
	19 mm	37,5 mm	19 mm	37,5 mm	
Poisson's ratio of concrete (μ)	0,15				
Subgrade modulus (k) (MPa/mm)	0,08				
Elastic modulus of concrete (E) (MPa)	21 000	29 000	41 000	48 000	24 000
Concrete slab thickness (h) (mm)	230				
Radius of relative stiffness (l) (mm)	722,4	783,1	853,9	888,2	746,9
Load radius (a) (mm)	95				
Load size ratio (a/l)	0,132	0,121	0,111	0,107	0,127

Figure 4.2 presents the joint shear stiffness calculated by using Equation B.44, the data presented in Table 4.2 and the LTE calculated from the laboratory deflections. For this particular figure only the static loading data has been plotted.

The unusual appearance of the plot for the 19 mm granite aggregate on a C rubber subbase under 20 kN load, shows the sensitivity of the parameter *AGG* to a change in LTE. The LTE for this particular test, presented on Figure 3.7, did not appear to vary that much. The LTE at 0,1 mm crack width was 96,4%,

from there it increased gradually to a maximum of 97,8% at a crack width of 0,5 mm. Although the difference in LTE was only 1,4%, the difference in *AGG* was more than 3 700 MPa.

The *AGG* values calculated for crack widths of 0,1 mm to 0,4 mm for the 37,5 mm granite aggregate are not shown on the graph, as the *AGG* increases rapidly the closer the LTE gets to a 100%. This is the region where the LTE approximates the upper asymptote, as shown on Figure 2.19. For a LTE of 99,2 % the *AGG* was calculated as 30 284 MPa.

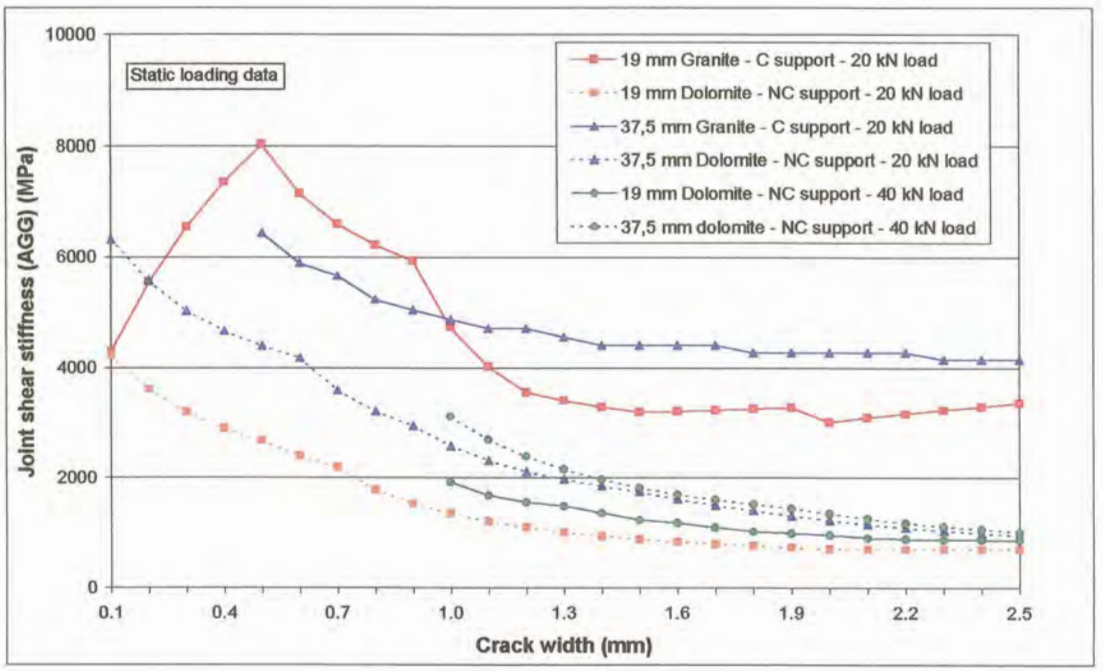

Figure 4.2: Joint shear stiffness versus crack width for static loading LTE results of aggregate interlock experiments

Generally the trends in the data were logical, with the 37,5 mm coarse aggregate having higher joint shear stiffnesses than the 19 mm coarse aggregate for the same subbase support and loading conditions. The 40 kN loading results were also higher than the 20 kN loading results, indicating that the heavier "action" required a greater "reaction" to resist it.

Figure 4.3 presents the joint shear stiffness values calculated for the static loading LTE of the plastic joint under both 20 kN and 40 kN loading.

Figure 4.3 further illustrates the influence of the subbase support on the behaviour of the joint. The C rubber subbase supported the slab to such an extent that initial shear stiffness results similar to that of the 19 mm coarse aggregate were calculated. Due to the smoothness of the plastic joint face the *AGG*, however, decreased quickly to a crack width of 0,7 mm where after it gradually increased again. As has been mentioned before, the response of the plastic joint, itself, were the results measured up to a

crack width of 1,5 mm, where after the response of the subbase was measured. It is also suspected that during this particular experiment the C rubber was pulled tight during crack opening, which explains the increase in LTE noticed earlier, as well as the increase in shear stiffness, at crack widths larger than 1,5 mm.

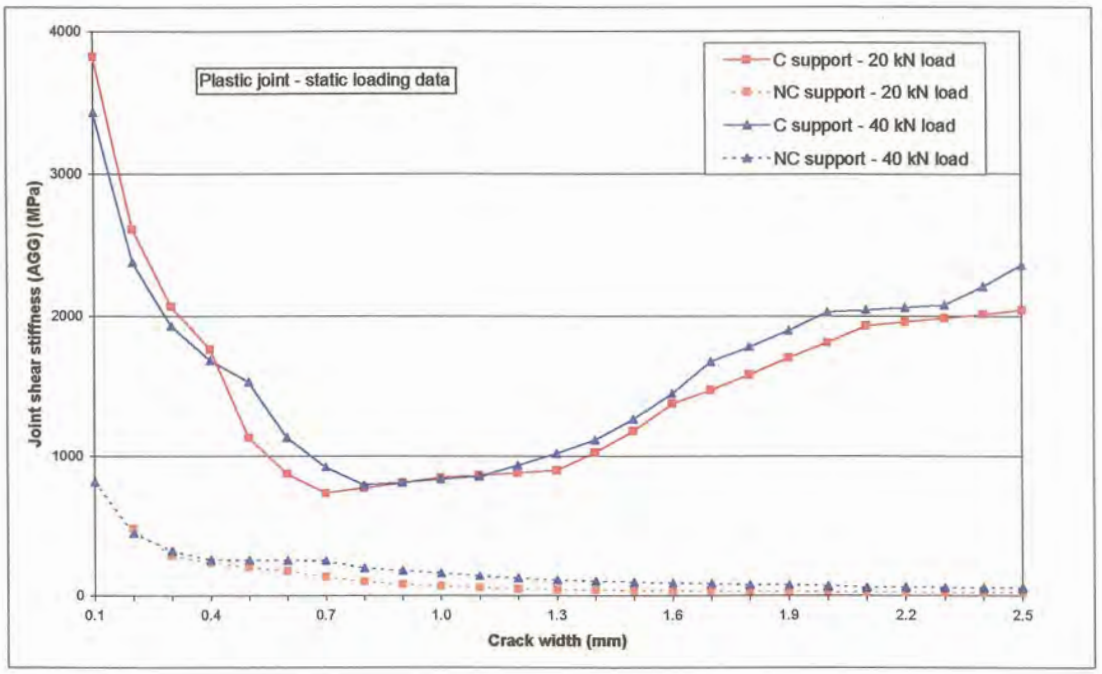

Figure 4.3: Joint shear stiffness versus crack width for static loading LTE results of the plastic joint

On the DC rubber support, on the other hand, the shear stiffness values were particularly low as could be expected from a smooth joint face. Of particular interest, is the fact that the shear stiffness calculated from the 40 kN load LTE values was approximately twice that of the 20 kN load LTE values. Once again showing that the larger "action" required a larger "reaction" in return. This was contrary to the results of for example the Endurance Index (EI), developed using rounded natural gravel, where doubling the load halved the EI (Colley and Humphrey, 1967).

An attempt has also been made to use the calculated joint shear stiffness to quantify the effect of dynamic loading versus static loading, as the difference in *AGG* results was more pronounced than the difference in LTE results. There was however no definite relationship that could be established in this instance. The only fact that can be stressed is that the *AGG*, just as the LTE, was higher under dynamic loading than under static loading. The average percentage increase in the *AGG* under dynamic loading over static loading, due to the effects of momentum, for the four aggregate interlock experiments is summarised in Table 4.3.

Table 4.3: Average increase in *AGG* due to dynamic loading

Experiment number	Aggregate size and type	Subbase	Increase in *AGG* due to dynamic loading (%)
1	19 mm granite	C rubber	128
2	37,5 mm granite	C rubber	183
3	19 mm dolomite	DC rubber	270
4	37,5 mm dolomite	DC rubber	282

The results in Table 4.3 indicated that the *AGG* under dynamic loading was approximately 1,5 times that of the *AGG* under static loading on the C rubber subbase, and approximately 3 times higher on the DC rubber subbase. The effect of different types of loads on the sound (C rubber) subbase is therefore not as big as the effect on the "weaker" (DC rubber) subbase. The further practical implication of this is that the forces induced in the pavement due to fast moving dynamic loads are able to "bridge" the discontinuities in the "weaker" (DC rubber) subbase with little detriment (small RM) to the pavement structure. But, the opposite is also true and that is that especially the vertical shear forces induced in the pavement due to slow moving heavy vehicles have a large detrimental effect (large RM) on the pavement with the "weaker" subbase.

4.3 ANALYSIS OF FIELD DATA

In practice concrete pavements are designed for a structural service life of up to 30 years (TRH4, 1985). The thickness of a specific pavement is mainly determined by future traffic projections, the quality of road construction materials and subgrade conditions. Therefore, when comparing the four road sections, discussed above, there are certain aspects that need to be highlighted. To facilitate the comparison the joint and mid-slab deflections, the RM and the LTE at joints, as well as the calculated remaining lives of each road section have been summarised in Table 4.4.

Table 4.4: Summary of FWD test results for all road sections

Road Section	40 kN Deflection (mm)				RM at joint (mm)	LTE at joint (%)	RM (years)
	Joint		Mid-slab				
	Average	Standard deviation	Average	Standard deviation			
1	0,250	0,047	0,116	0,043	0,07–0,26	44	4
2	0,101	0,058	0,083	0,038	0,00–0,19	76	14
3	0,225	0,097	0,091	0,057	0,06-0,12	67	6
4	0,157	0,088	0,059	0,026	0,03-0,20	84	20

At the time of investigation, the ages of the four pavements were 32, 14, 23, and 13 years, respectively. The fact that Road Section 1 had a RM of only 4 years maximum could be expected, as it was older than 30 years. Road Section 1 also had the highest average mid-slab and joint deflection values, with the lowest LTE at the joints.

When comparing Road Sections 2 and 4, which were constructed at approximately the same time, and carried the same amount of traffic, it could have been expected that their remaining lives would be the same. The concrete pavement on Road Section 2 was an overlay on an existing asphalt pavement. The subbase beneath the concrete of Road Section 2 was therefore more elastic than the cement stabilised subbase beneath the concrete pavement of Road Section 4. The result of this was lower deflections and RMs for the former than for the latter at the joints, but higher mid-slab deflections. Other factors that contributed to the lower RM of Road Section 2 were poorer subgrade conditions, and a wetter climate subjecting the pavement to chemical weathering processes.

In terms of design age and RM, it could be expected that Road Section 3 would still have a structural capacity of 8 to 10 years. However, the no-fines subsoil drain between the concrete pavement and the asphalt shoulder, as well as the asphalt shoulder, itself, did contribute to a reduction in the RM, and to the fact that the pavement already received a SAMI.

4.3.1 Relative movement analysis

The pavement models derived through back-calculation of the field investigation data of the four road sections were analysed using the software package, EverFE. The main purpose in this theoretical analysis was to demonstrate the difference between the RMs measured, using the FWD and the actual RMs across the joint itself. The reason for this is that the FWD measures the deflection at a point in the centre of the load, next to a joint, with the first geophone with which the RM is determined situated 200 mm away on the other side of the joint. During the laboratory experiments, on the other hand, the LVDT's measuring RM across the crack were situated as close as possible to the edge of the crack, and on opposite sides of the crack.

For comparison purposes the RMs were therefore determined theoretically beneath the load, on both sides of the joint, and 200 mm away from the centre of the load, on the opposite side of the joint. The results are plotted on Figures 4.4 to 4.7. The vertical axes of the graphs on these figures have been kept the same to facilitate an easier comparison of the deflection behaviour of the four different road sections.

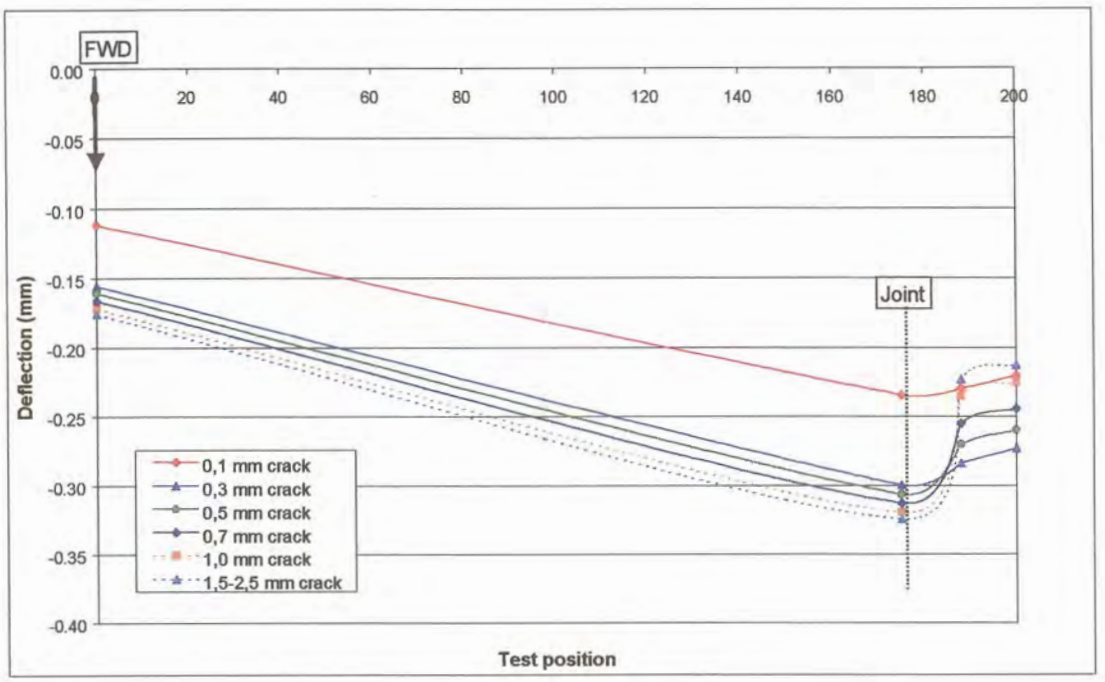

Figure 4.4: Simulated deflection across joint – Road Section 1

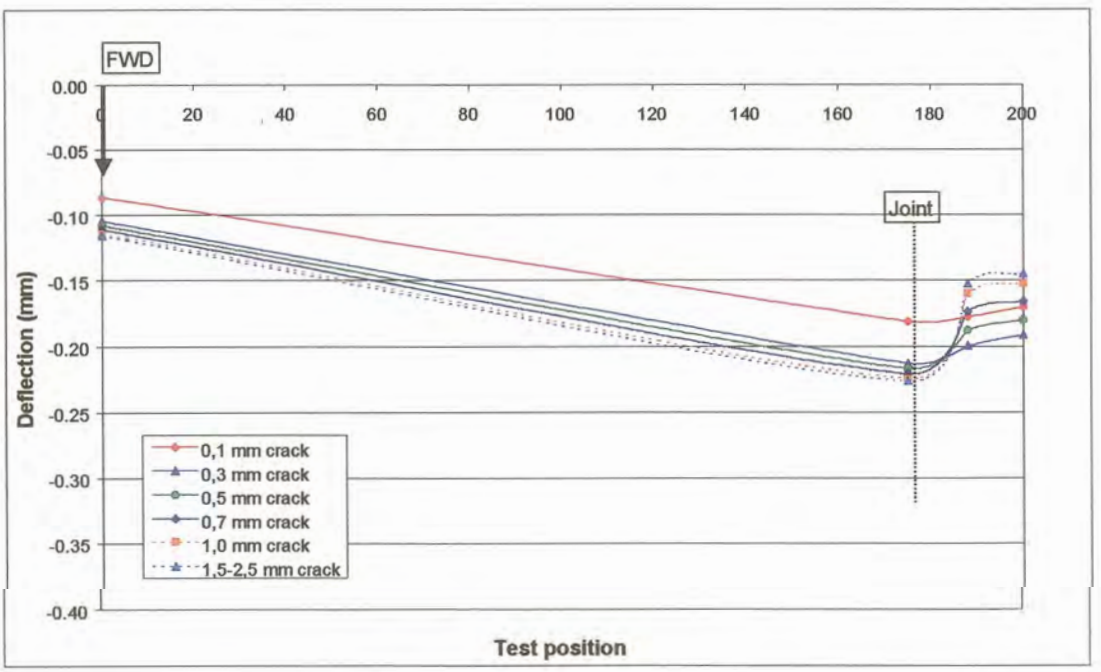

Figure 4.5: Simulated deflection across joint – Road Section 2

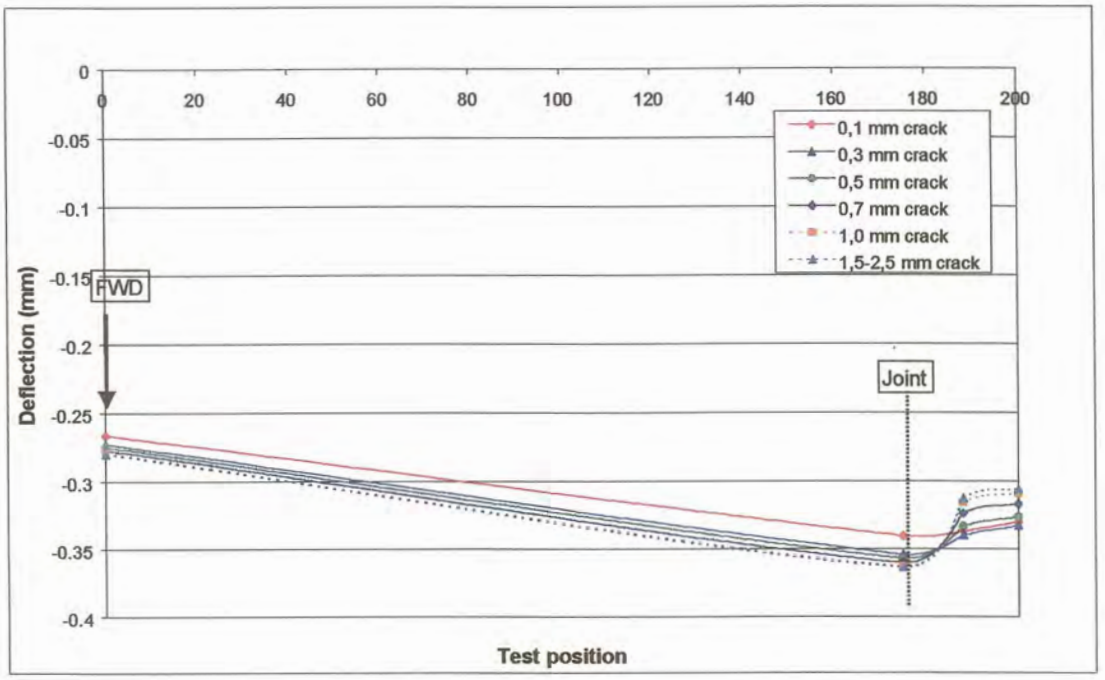

Figure 4.6: Simulated deflection across joint – Road Section 3

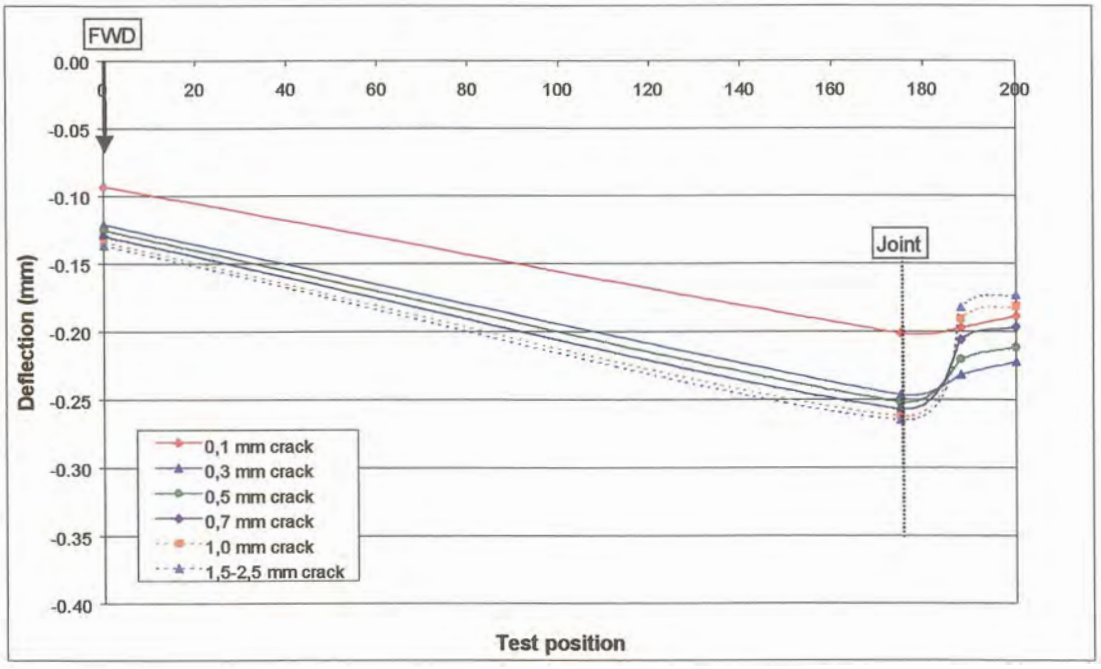

Figure 4.7: Simulated deflection across joint – Road Section 4

At narrow crack widths, the RM between the load position and the first geophone, 200 mm away, was larger than the RM across the joint. However, at crack widths between 0,7 mm and 1,0 mm, with the crack opening up and the LTE decreasing, the leave slab was pressed down further relative to the approach slab, the RM was reversed with the RM directly across the joint larger than the RM at 200 mm from the load position.

According to the theoretical analysis, Road Section 3 has the highest deflections, followed by Road Section 1, and Road Section 4, with Road Section 2 having the lowest deflections. The shape of the deflection curve was also influenced by the assumption that FWD testing would normally be conducted during the daytime, while the temperature of the concrete surface is typically 10°C greater than at the bottom. From there the upward curled shape of the slab from the joint position to the FWD load position. The distance between the deflection measurement at the joint, and the next point across the joint, is to allow for the reamed width at the top of the joint.

4.3.2 Aggregate interlock joint/crack shear stiffness

Similar to the analysis done for the laboratory data, the aggregate interlock joint shear stiffness was also determined. The relationship between deflection LTE and the dimensionless joint stiffness (AGG/kl) developed by Ioannides and Korovesis (1990) was used to calculate the shear stiffness per unit length (AGG) of the crack faces of the experimental slabs. The LTE calculated from the field data, together with Equation B.44 (Appendix B) was used. The values used in the calculation of the shear stiffness are summarised in Table 4.5.

Table 4.5: Input values for calculating shear stiffness (AGG) of crack faces

Description	Road Section			
	1	2	3	4
Poisson's ratio of concrete (μ)	0,15			
Subgrade modulus (k) (MPa/mm)	0,10	0,085	0,10	0,12
Elastic modulus of concrete (E) (MPa)	35 000	37 000	24 000	35 000
Concrete slab thickness (h) (mm)	200	230	210	210
Radius of relative stiffness (l) (mm)	699,0	819,7	659,8	692,7
Load radius (a) (mm)	135			
Load size ratio (a/l)	0,193	0,165	0,205	0,195

For Road Section 1 the LTE data in Table 3.4 was used, but for Road Sections 2, 3 and 4, the LTE from the original database was used. The graph presented in Figure 4.4 (Ioannides and Korovesis, 1990) was

used as the basis for the comparison, but in order to distinguish between the Road Sections, only the *AGG* values were plotted on a logarithmic scale on the X-axis and not *AGG/kl* (see Figure 4.8).

With the LTE data varying from nearly 0% to 100%, it was logical that the AGG values would also vary greatly. As can be seen from Figure 4.8 the AGG varied from approximately 4 MPa to 22 400 MPa. However, it was still possible to distinguish that the joint stiffness, calculated from the structural characteristics of the individual road sections, indicated that the road section with the highest RM (Road Section 4), also had the highest joint stiffness for a specific LTE. Simultaneously Road Section 3 had the lowest *AGG*, with Road Section 2 plotting in between. The values plotted for Road Section 1 were too little to draw a conclusion. This trend in the data was similar to the RM results presented in Table 4.4, above.

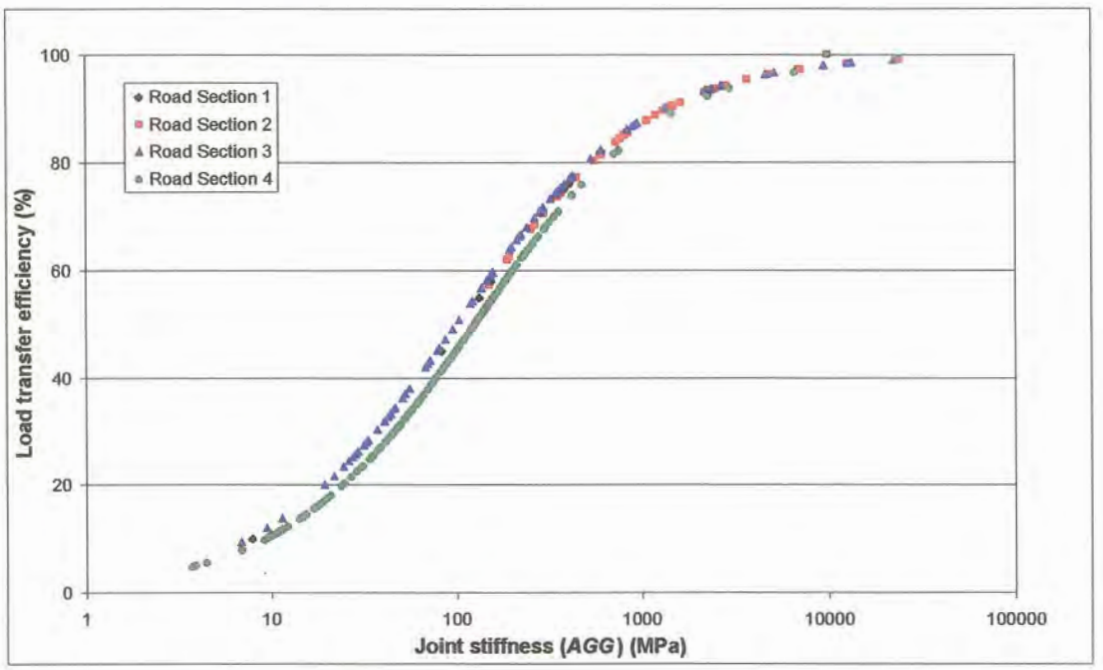

Figure 4.8: LTE versus joint stiffness calculated for field data

4.3.3 South African mechanistic concrete pavement design software

4.4 CONCLUSIONS

During the laboratory studies conducted for this research project, an attempt was made to reach a better understanding of the intricacies involved in defining the mechanism of aggregate interlock. This mechanism can only be understood adequately if it is borne in mind that normal stress, shear stress,

crack width, and shear displacement are all involved. On the other hand, concrete strength, aggregate size, and subbase support also influenced the results.

Tests on cracks subjected to earthquake loading Walraven (1981) showed that there is a considerable difference between the first and the subsequent loading cycles. Irreversible damage to the cement matrix takes place when the hard aggregate particles are pushed into this softer cement matrix. Any new cycle of loading leads to further damage of the crack faces, resulting into steadily increasing values of the shear displacement and the crack width at peak loading. In effect this was also proven during this study. The load applied to induce the crack in the less than 24-hour old concrete can be described as the first loading cycle, during which irreversible damage took place, in other words, during which the crack was formed. Subsequent loading and opening and closing of the crack caused further damage and the dislodging of fine particles in some instances that prevented the closing of the crack back to 0,1 mm once it has been pulled open.

Yet, despite this "damage" to the crack faces, the results obtained using the high quality crushed stone found in South Africa were superior to results obtained using USA aggregates. The common practice in South Africa of constructing jointed concrete pavements without dowels at the joints relying on aggregate interlock load transfer only has therefore been vindicated by this study.

The main contribution to the current state of knowledge was the development of a mechanistic equation quantifying the effect of aggregate interlock at a joint/crack in a concrete pavement. This equation has already been included and tested in the CncRisk software package, developed as part of the upgrading of the new mechanistic concrete pavement design manual for Southern Africa.

The structural performance of four different road sections was analysed in this chapter. The pavements were analysed by comparing the existing pavement designs, results of field investigations, and the structural RM of each.

At the time of investigation, the ages of Road Sections 1 to 4 were 32, 14, 23, and 13 years, respectively. Road Section 1 had a RM of only 4 years maximum, which could be expected, as it was older than 30 years. Road Section 1 also had the highest average mid-slab and joint deflection values, with the lowest LTE at the joints.

Road Sections 2 and 4 were constructed at approximately the same time, and carried the same amount of traffic, and it could have been expected that their remaining lives would be the same. But, the concrete pavement on Road Section 2 was an overlay on an existing asphalt pavement. The subbase beneath the concrete of Road Section 2 was therefore more elastic than the cement stabilised subbase beneath the concrete pavement of Road Section 4. The result of this was lower deflections and RMs for the former than for the latter at the joints, but higher mid-slab deflections. Other factors that

contributed to the lower RM of Road Section 2 were poorer subgrade conditions, and a wetter climate subjecting the pavement to chemical weathering processes.

The aggregate interlock joint shear stiffness was determined for each road section through the process developed by Ioannides and Korovesis (1990). The joint stiffness, calculated from the structural characteristics of the individual road sections, indicated that the road section with the highest RM (Road Section 4), also had the highest joint stiffness for a specific LTE. Simultaneously Road Section 3 had the lowest *AGG*, with Road Section 2 plotting in between. This was similar to the RM results presented in Table 4.4, above.

CHAPTER 5: APPLICATION OF LABORATORY AND FIELD MODELLING

TABLE OF CONTENTS

		Page
5	**APPLICATION OF LABORATORY AND FIELD MODELLING**	**5-1**
5.1	**INTRODUCTION**	**5-1**
5.2	**AGGREGATE INTERLOCK FORMULA FOR SOUTH AFRICAN MECHANISTIC CONCRETE PAVEMENT DESIGN MANUAL**	**5-1**
5.2.1	Laboratory data	5-1
5.2.2	Field data	5-3
5.3	**RELATIVE MOVEMENT VERSUS LOAD TRANSFER EFFICIENCY**	**5-4**
5.4	**SUMMARY**	**5-9**

LIST OF TABLES

Table 5.1: Comparison between "before" and "after" CncRisk analyses 5-3
Table 5.2: Summary statistics of LTE and RM data for Road Sections 2, 3 and 4 5-6

LIST OF FIGURES

Figure 5.1: Input detail for Main Control Panel 5-2
Figure 5.2: Graphic illustration of improvement to aggregate interlock equation 5-3
Figure 5.3: RM versus LTE for Road Sections 2, 3 and 4 5-5
Figure 5.4: RM versus LTE – comparison between laboratory and field data 5-6
Figure 5.5: RM versus LTE – relationship between laboratory data and Road Section 4 5-7
Figure 5.6: RM versus LTE – relationship between laboratory data and average of field data 5-8

LIST OF SYMBOLS / ABBREVIATIONS

agg	Nominal size of 20% biggest particles in concrete mix
C	Continuous
DC	Discontinuous
$E_{subbase}$	Subbase stiffness modulus
F	Shift factor
k	Subgrade modulus
l	Radius of relative stiffness

LTE	Load transfer efficiency
RM	Relative movement
v	Vehicle speed
x	Crack width
y(x)	Relative vertical movement

5 APPLICATION OF LABORATORY AND FIELD MODELLING

5.1 INTRODUCTION

The primary objectives of this thesis have been achieved. This has been done through a detailed literature survey in order to lend guidance to the research and laboratory modelling conducted for this thesis and a thorough analysis of laboratory and field data. But not only that, insight has also been gained in the relationship between relative movement and load transfer efficiency of laboratory and field data through the development of a shift factor to fit the laboratory data to specific field data sets. The details are discussed below.

5.2 AGGREGATE INTERLOCK FORMULA FOR SOUTH AFRICAN MECHANISTIC CONCRETE PAVEMENT DESIGN MANUAL

5.2.1 Laboratory data

Reference has been made to the fact that the research done for this thesis formed part of the overall process of producing a new mechanistically based concrete pavement design manual for South Africa. The software package CncRisk has been developed as part of the new design manual. However, the original software still contained Equation (2.12) for the calculation of the aggregate interlock factor, Ca, referred to by Strauss et al. (2001). The RM data calculated from the deflections was used to develop a single equation to replace Equation (2.12) in the source code of the software package. A Weibull probability density function was generated, as follows:

$$y(x) = 0{,}118(1 - e^{-((v + \frac{11{,}413}{agg})x)^{1{,}881}}) \qquad (5.1)$$

Where:

$y(x)$	=	Relative vertical movement at joint/crack (mm);
v	=	0,136 for static loading (speed = 0 km/h);
	=	0,035 for dynamic loading (speed = 80 km/h);
x	=	Crack/joint width (mm); and
agg	=	Nominal size of 20% biggest particles in concrete mix (mm).

So-called "before" analyses were conducted with the original version of the software, containing Equation (2.12). For the input on the Main Control Panel of the software, typical jointed concrete pavement parameters were used (see Figure 5.1). The variation in the theoretical expected life of the pavement with 19 mm and 37,5 mm aggregate sizes, at specific crack widths was determined. Actual relative movements measured at specific crack widths during the laboratory studies were used.

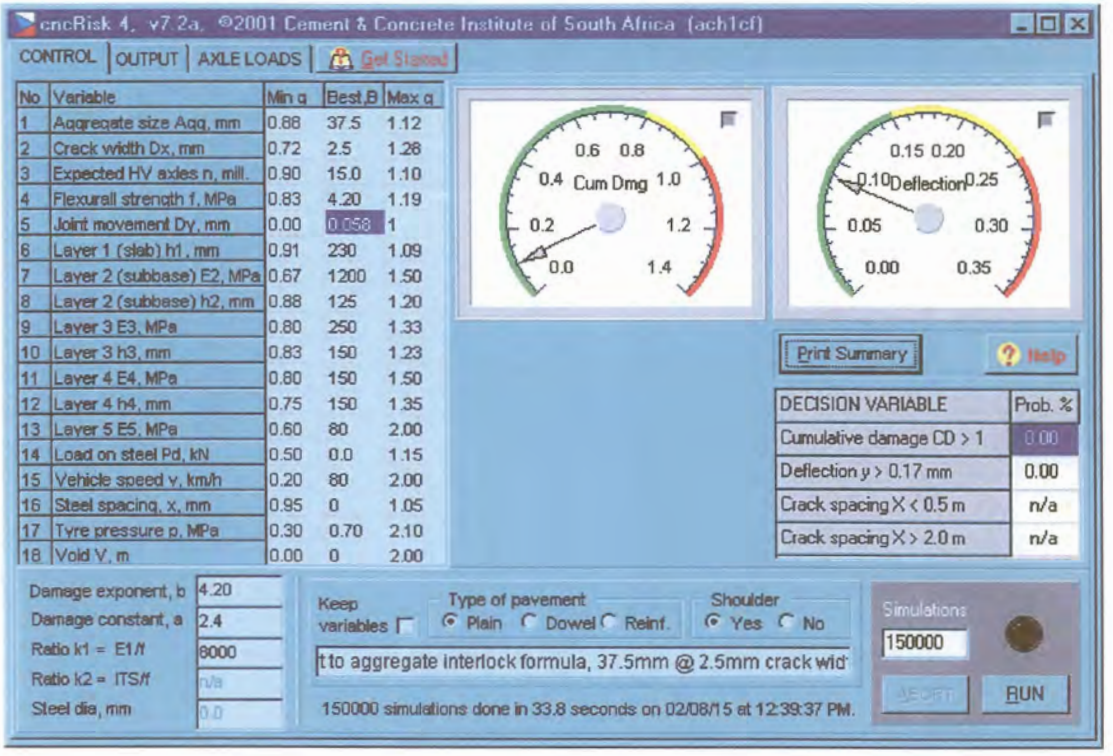

Figure 5.1: Input detail for Main Control Panel

Equation (5.1) was then included in the source code, and the same sets of input data re-used to conduct "after" analyses with the revised version of the software. The results of these "before" and "after" analyses are summarized in Table 5.1.

The discrepancy in Equation (2.12) for the smaller 19 mm sized aggregate, illustrated in Figure 3.15, was confirmed, by the fact that the expected life calculated through the software increased with increasing crack width, and relative movement during the "before" analyses. This is contrary to what physically happens in a concrete pavement where the life decreases with an increase in crack width and relative movement. The results for the larger 37,5 mm sized aggregate were more realistic, decreasing with an increase in crack width and relative movement. The pavement life calculated after the inclusion of Equation (5.1) decreased with increasing crack width and relative movement, for both aggregate sizes. The pavement life was also higher for the 37,5 mm aggregate concrete than for the 19 mm aggregate concrete. The results obtained were for illustration purposes, and should not be taken as absolute values

However, a more practical method to illustrate the contribution of the newly developed Equation (5.1) is to graphically illustrate the adjustment in the line plotted with the previous Equation (2.12) versus this new equation. This is shown on Figure 5.2.

Table 5.1: Comparison between "before" and "after" CncRisk analyses

Aggregate size (mm)	Crack width (mm)	Relative movement (mm)	Pavement Life (N x 10^6)	
			Before	After
19	1,0	0,040	46,6	52,6
	2,0	0,092	50,7	48,7
	2,5	0,100	55,1	48,0
37,5	1,0	0,015	54,0	58,2
	2,0	0,042	47,8	52,8
	2,5	0,058	46,8	51,3

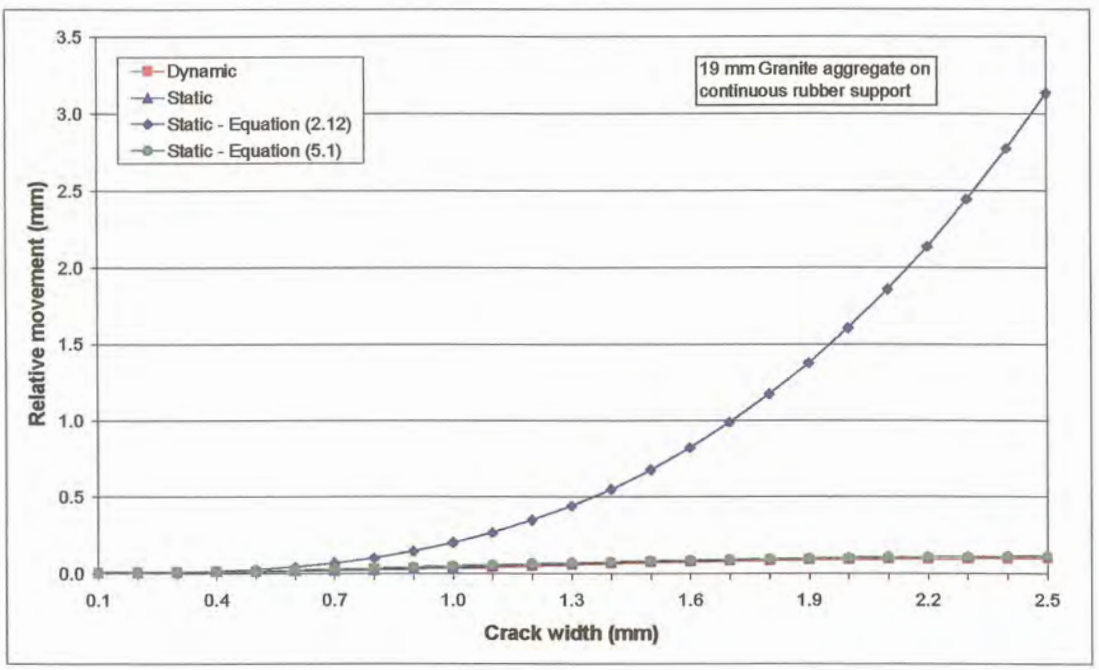

Figure 5.2: Graphic illustration of improvement to aggregate interlock equation

From Figure 5.2 it is obvious that there is little difference between the results measured in the laboratory and the results calculated with Equation (5.1).

5.2.2 *Field data*

In paragraph 3.4.2, it was mentioned that the original version of the CncRisk software was used to calculate the RM of Road Section 1. After inclusion of Equation (4.1) in CncRisk, all four road sections were analysed again. The laboratory data indicated that at a relative movement of approximately 0,12 mm, the crack width was 2,5 mm. Bearing this in mind and to be a bit more

optimistic, it was decided to set the crack width at 2,0 mm with a RM of 0,12 mm. The void length was set at 1,0 m. The pavement layer thicknesses and back-calculated stiffness moduli presented in the previous paragraphs were used. The vehicle speed was set at 0 km/h to be on par with the FWD test results. The projected heavy vehicles (E80's) over the remaining lives predicted from previous analyses (see Table 4.4) was 1,5 million for Road Section 1, 80 million for Road Section 2, 22 million for Road Section 3 and 68 million for Road Section 4.

The results were as follows:

a) Road Section 1 already showed cumulative damage of 27,5% with a RM of 0,8 million E80's at a crack width of only 0,5 mm and void length of 0 m. This confirmed that the pavement was already in a terminal condition and brought the RM down to only two years, which is half of what was calculated with the earlier version of CncRisk.

b) CncRisk confirmed that after 14 years the pavement of Road Section 2 will show cumulative damage of 10,5%, which is the maximum percentage damage allowed, before rehabilitation is required (Manual M10, 1995). The projected RM is 103 million E80's, which indicates that the pavement will still be in a reasonable condition, but will need attention.

c) The cumulative damage calculated for Road Section 3 was 54% with a RM of 11 million E80's (4 years) at a crack width of 2 mm, RM of 0,12 mm and void length of 1 m. This, according to CncRisk, is a clear indication that the pavement was already in a distressed state and needed attention. The repair work that has already been done on this road section was therefore necessary.

d) Given the projected traffic and back-calculated layer stiffness moduli, the cumulative damage calculated for Road Section 4 was 54% with a RM of only 33 million E80's (12 years) at a crack width of 2 mm, RM of 0,12 mm and void length of 1 m. This was far less than what has been predicted above. On the one hand the stiffness moduli may have been under-estimated, but with average deflections higher than that of Road Section 2, it may not be far off. This road section will have to be monitored closely.

These analyses have shown that the software package CncRisk is a handy tool to determine the RM of an existing pavement. Further investigation is required to determine the reason for the large difference in the result of Road Section 4.

5.3 RELATIVE MOVEMENT VERSUS LOAD TRANSFER EFFICIENCY

The original database for Road Sections 2, 3 and 4 was used to evaluate the RM versus the LTE calculated from the field data (the original data for Road Section 1 was not available). The data together with an exponential curve fitted through the points for each individual Road Section, is shown on Figure 5.3. These curves were all of the format $y(x) = 100e^{-Fx}$. With RM = 0 at LTE = 100%, the

intercept of all three curves was 100. The factor, F, was assumed to be a function of the subbase support, the radius of relative stiffness, as well as the subgrade k-modulus, which still had to be determined.

Contrary to the maximum RM of approximately 0,12 mm measured in the laboratory for the aggregate interlock experiments, values of up to 0,5 mm were measured in the field. In this instance, if LTE is considered to be indicative of the RM of a pavement, the RM versus LTE did not seem to correlate with the remaining lives already calculated. Of the three sections, Road Section 4 supposedly has the largest RM, but according to the exponential curve fitted to the data, it approximates a lower LTE at a RM of 0,5 mm than Road Section 3.

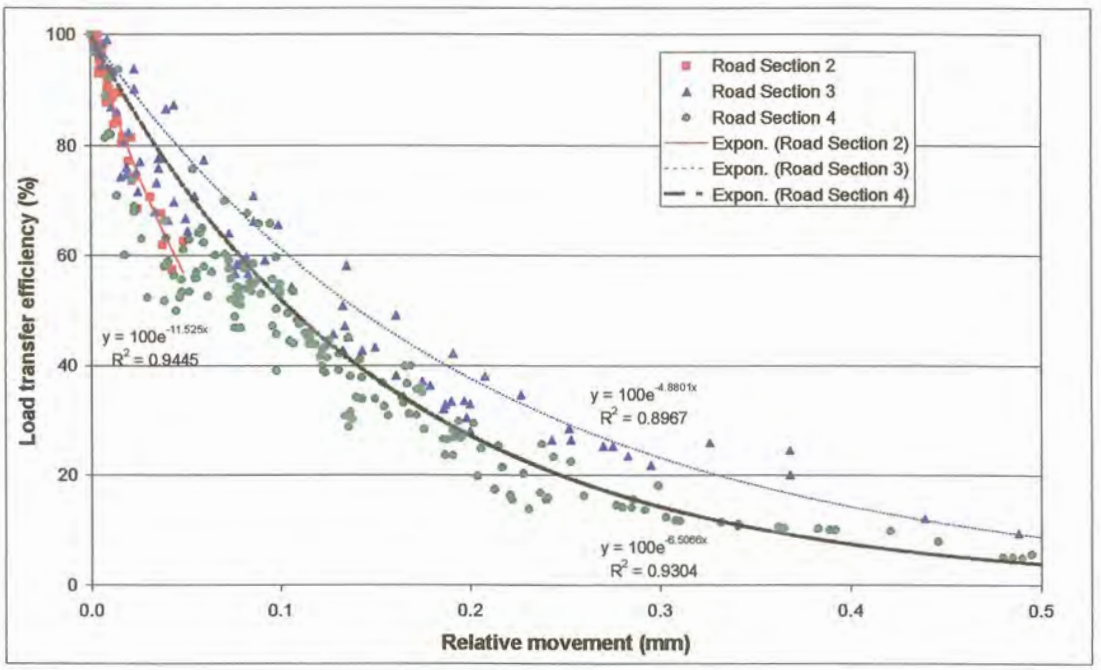

Figure 5.3: RM versus LTE for Road Sections 2, 3 and 4

Road section 3 with the lowest RM of the three sections considered showed the largest LTE. The amount of data available for Road Section 2 was little in comparison with Road Sections 3 and 4. Most of the LTE results for Road Section 2 were between 60% and 100%, with the maximum RM only 0,05 mm. A summary of the statistical parameters of the LTE and RM data for the three road sections is given in Table 5.2.

Table 5.2: Summary statistics of LTE and RM data for Road Sections 2, 3 and 4

Statistical parameter	Road Section 2		Road Section 3		Road Section 4	
	RM	LTE	RM	LTE	RM	LTE
Average	0,013	87,3	0,126	57,4	0,146	42,2
Standard deviation	0,012	11,5	0,120	25,5	0,109	20,6
Minimum	0,000	57.4	0,002	9,4	0,000	4,9
Maximum	0,049	100,0	0,586	99,0	0,495	100,0

Further to the above comparison, the field data was also used to calibrate the laboratory data (from Chapter 3). For this purpose, the 40 kN static loading data for the 19 mm and 37,5 mm coarse aggregates as well as for the plastic joint on the discontinuous subbase was used, as the combined results covered the same range of RM measurements as the field data (see Figure 5.4).

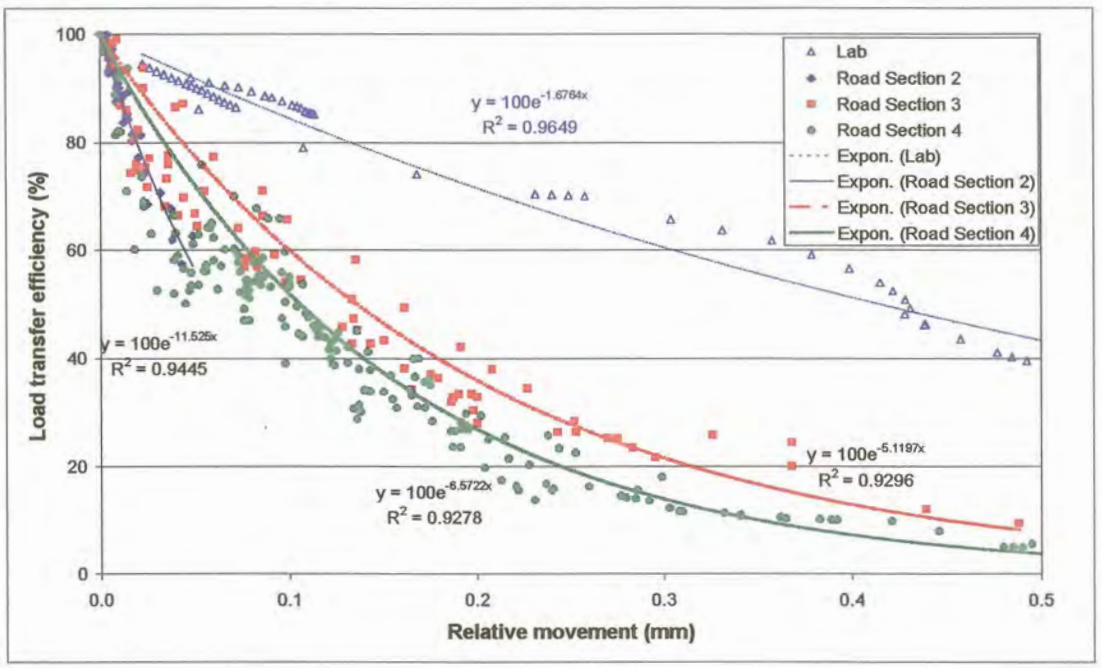

Figure 5.4: RM versus LTE – comparison between laboratory and field data

When analysing the results plotted on Figure 5.4, the sensitivity of the model developed in this thesis can be summarised as follows:

a) The larger the crack width, the greater the RM.

b) The greater the vehicle speed, the smaller the RM.

c) The larger the aggregate size, the smaller the RM.

d) The higher the elastic modulus of the concrete the smaller the RM for the same LTE.

e) The higher the elastic modulus of the subbase, the smaller the RM, also for the same LTE.

In order to calculate a "shift" factor between the laboratory and field data, an exponential curve was fitted through the laboratory data as well. The values calculated with the exponential fit for the laboratory data was then divided by the comparative values for the field data of each road section. The relationships between each of the field data sets and the laboratory data set were also exponential curves (with $R^2 = 1$), which increased with increasing crack with. For example, LTE (Lab/Road Section 4) = $100e^{-1.6764RM}/100e^{-6.5722RM} = e^{4.8958RM}$. This is illustrated in Figure 5.5, where the laboratory and Road Section 4 data were compared. The relationship Lab/Road Section 4 with the exponential curve fitted through it, is also plotted on Figure 5.5. The curve F4 was obtained by dividing the curve fitted through the laboratory data by the curve fitted through the relational curve, in other words $100e^{-1.6764RM}/e^{4.8958RM}$. This implied that in order to "shift" the laboratory data to either of the field data sets, the RM-coefficient (F) of the relational curve had to be established for each data set.

Various combinations of the subgrade modulus (k), radius of relative stiffness (l) and the subbase stiffness ($E_{subbase}$) were used. For the equation $LTE = e^{F*RM}$, the combination that gave the closest results for the shift factor (F) was:

$$F = l/(k*E_{subbase}) \quad (5.2)$$

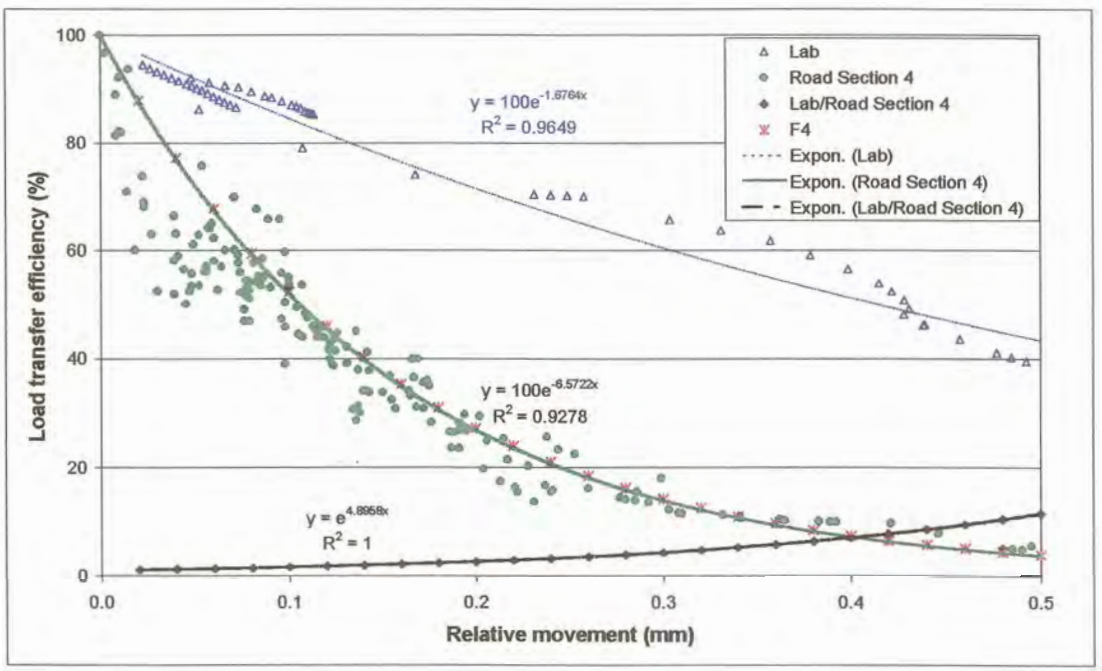

Figure 5.5: RM versus LTE – relationship between laboratory data and Road Section 4

The F of the exponential curve fitted to the laboratory data in effect already incorporated these three parameters as an inherent characteristic. It was therefore logical that these three parameters would also contribute to the shift in data. The shift factor by itself has the units mm^2/MPa^2, which is a surface area over a surface stress. When, however the exponential curve fitted to the laboratory data is divided by the shift factor, the units are cancelled out, making it dimensionless.

Another important aspect that has to be emphasised here and which the range achieved in the laboratory RM shows, is that the RM over which aggregate interlock plays the primary role in load transfer, varies from approximately 0 mm to 0,12 mm. At larger RMs the subbase influenced the results to a great extent, which is clearly shown by the RM of the smooth plastic joint. This was also one of the main reasons for including the stiffness modulus of the subbase during determination of the F-factor.

To test whether this shift factor would apply to any data set, the results of the three road sections were combined into one set of data and an exponential curve fitted through it. The average k, l and $E_{subbase}$ of the three road sections was calculated and used as the x-coefficient to plot curve F in Figure 5.6. It was remarkably close to the exponential curve fitted to the field data.

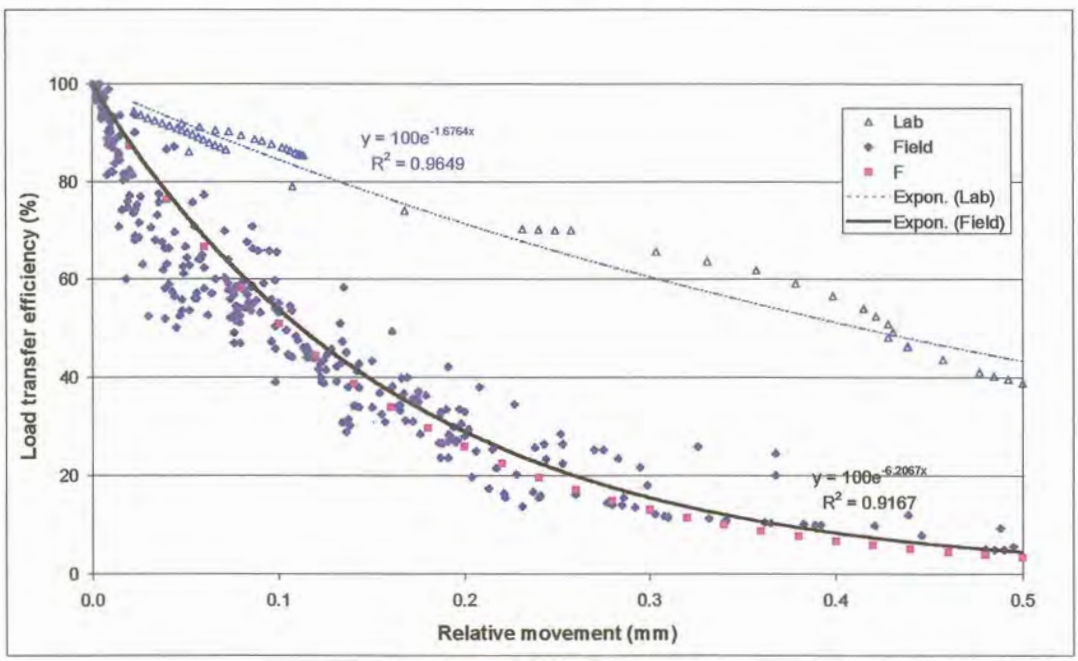

Figure 5.6: RM versus LTE – relationship between laboratory data and average of field data

Where the RM in the field is larger than 0,12 mm, two main assumptions can be made from this comparison between the laboratory and the field data, namely:

a) The aggregate interlock capacity of the crack face, itself is still intact, but the crack width is larger than 2,5 mm, or

b) The crack face has been eroded due to traffic loading to such an extent, that the crack face has become smooth, and has little aggregate interlock capacity.

Bearing in mind the high quality of the crushed stone in South Africa, the first of the two assumptions seems to be the more likely option.

5.4 SUMMARY

The main contribution to the current state of knowledge was the development of a mechanistic equation quantifying the effect of aggregate interlock at a joint/crack in a concrete pavement. This equation has already been included and tested in the CncRisk software package, developed as part of the upgrading of the new mechanistic concrete pavement design manual for Southern Africa. Furthermore, application of the revised version of the CncRisk software that included Equation (5.1) mostly confirmed the remaining lives of the road sections as predicted by different individuals in the reports used to compile the field investigation data.

The RM and LTE data from three of the four road sections was used to calibrate the laboratory data. The calibration factor was a function of the subgrade modulus (k), radius of relative stiffness (l) and the subbase stiffness ($E_{subbase}$). In effect this calibration of the data has also shown that one of the main objectives of the particular test set-up used for the aggregate interlock experiments has been achieved in that the RM range over which load transfer is enabled due to aggregate interlock of the 19 mm coarse aggregate could be established. Indications are however; that for larger 37,5 mm coarse aggregates this range extends past the values tested. The main contribution of the plastic joint results in combination with the aggregate interlock results, was that the same range of RM measurements as the field measurements was obtained. This therefore clearly indicated where the LTE measured in the field, relies mainly on the subbase stiffness, due to either crack widths larger than 2,5 mm, or an aggregate crack face that has been abraded under traffic movement to such an extent that it gives the same relative movement results as a smooth joint.

The sensitivity of the model developed in this thesis can be summarised as follows:

a) *The larger the crack width, the greater the RM.*

b) The greater the vehicle speed, the smaller the RM.

c) The larger the aggregate size, the smaller the RM.

d) The higher the elastic modulus of the concrete the smaller the RM for the same LTE.

e) The higher the elastic modulus of the subbase, the smaller the RM, also for the same LTE.

CHAPTER 6: SUMMARY, CONCLUSIONS AND RECOMMENDATIONS

TABLE OF CONTENTS

		Page
6	**SUMMARY, CONCLUSIONS AND RECOMMENDATIONS**	**6-1**
6.1	**SUMMARY**	**6-1**
6.1.1	Aggregate interlock	6-1
6.1.2	Dowel modelling	6-3
6.1.3	Field investigation	6-3
6.2	**CONCLUSIONS**	**6-4**
6.3	**RECOMMENDATIONS**	**6-6**
6.3.1	Follow-up testing	6-7

LIST OF SYMBOLS / ABBREVIATIONS

agg	Nominal size of 20% biggest particles in concrete mix
$E_{subbase}$	Subbase stiffness modulus
F	Shift factor
k	Subgrade modulus
l	Radius of relative stiffness
LTE	Load transfer efficiency
RM	Relative movement
v	Vehicle speed
x	Crack width
y(x)	Relative vertical movement

6 SUMMARY, CONCLUSIONS AND RECOMMENDATIONS

6.1 SUMMARY

6.1.1 Aggregate interlock

The primary objective of this study was to investigate existing methods for modelling aggregate interlock shear transfer across a joint in a concrete pavement, and to develop a model that reflects variations in joint load transfer with joint opening, load magnitude and concrete properties. It was envisaged that this model / equation could replace an existing equation as part of the upgrading of the south African concrete pavement design manual to a manual based on mechanistic design principles. During a process of investigating the background of concrete pavements constructed in South Africa, defining the rigid pavement system, investigating historical developments in concrete pavement design, and a thorough literature review, this objective has been explored.

The software package EverFE (Davids et al, 1999) was used to do theoretical modelling, and to determine the accuracy of equipment required for experimental modelling. Part-slab studies were conducted inside a laboratory to reduce the effect of temperature variations on the test set-up, as well as eliminate exposure of the slab to environmental influences such as direct sunlight, and/or rain. Instrumentation included thermocouples to collect slow responses due to environmental influences. Linear variable displacement transducers (LVDT's) and strain displacement transducers collected fast responses induced by dynamic and static loads. The testing also included determining the relevant engineering properties for South African concrete aggregates.

The experimental programme was set up according to a 2-level, 2-parameter design. The aggregate types chosen were Granite with an E-modulus of 27 GPa (Aggregate crushing value (ACV) = 27%), and Dolomite with an E-modulus of 40 GPa (ACV = 15%), representing the range in modulus of crushed aggregates used in the construction industry in South Africa. To cover the spectrum of aggregate sizes used in the construction of concrete, 19 mm as well as 37,5 mm coarse aggregates were used. Four concrete slabs were cast to determine the effects of aggregate interlock, as follows:

a) Experiment 1 – 19 mm granite aggregate.
b) Experiment 2 – 37,5 mm granite aggregate.
c) Experiment 3 – 19 mm dolomite aggregate.
d) Experiment 4 – 37,5 mm dolomite aggregate.

A fifth concrete slab with a pre-deformed plastic joint former was cast to investigate the performance of a different type of joint under both dynamic and static loading. This slab was used to quantify the difference between a continuous and a discontinuous Winkler subbase and also to complete the data in the relative movement (RM) and LTE analysis..

The response of the experimental slabs was captured under moving impulse or dynamic loading (equivalent to traffic loading) as well as under static loading to be able to capture real-life conditions and to compare the results. An impulse force that simulates the impact of one wheel (20 kN) of a standard 80 kN dual wheel axle load, crossing a joint/crack at 80 km/h was developed. The impulse force was applied across the crack formed in the slab (within 24 hours after casting) by means of two actuators at a frequency of 3 Hz for 2 million load cycles each on the slabs cast for Experiments 1 and 2. During Experiment 1 it became apparent that even the weaker of the two aggregate types, namely granite, experienced no significant deterioration inside the crack face at the initial crack width up to 2 million dynamic load cycles. This could be attributed to the fact that both the cement paste and aggregate particles were so tightly knit together at the initial crack width that little vertical sliding could occur. This indicated that little abrasion of the aggregates at the joint face took place at the initial crack width, as the narrow crack restricted vertical shear movement, and that the shear stress developed within the crack face was too low for fatigue to take place. Therefore no loose particles were dislodged, or got trapped in a different position when the crack opened and closed. This could also be attributed to the high quality of crushed stone used in South Africa. This was confirmed by subjecting Experiment 2 to 2 million dynamic load cycles as well, and confirming that the deflections measured, as well as the LTE calculated stayed constant during the full loading cycle.

Experiments 1 and 2 were constructed on continuous rubber support layers, whereas for Experiments 3 and 4, the top rubber layer was cut through right beneath the crack, to simulate a crack propagating into the subbase. Both of these subbases represented a liquid (Winkler) foundation, for the first two experiments it was continuous, and for the latter two, discontinuous.

The RM data calculated from the deflections was used to obtain an equation to replace a previous, inaccurate equation in the source code of the software package CncRisk (written as part of the development of a new South African mechanistic concrete pavement design method). A Weibull probability density function was generated, as follows:

$$y(x) = 0{,}118(1 - e^{-((v + \frac{11{,}413}{agg})x)^{1{,}881}}) \tag{6.1}$$

Where:

$y(x)$	=	Relative vertical movement at joint/crack (mm);
v	=	0,136 for static loading (speed = 0 km/h);
	=	0,035 for dynamic loading (speed = 80 km/h);
x	=	Crack/joint width (mm); and
agg	=	Nominal size of 20% biggest particles in concrete mix (mm).

The sensitivity of the model developed in this thesis can be summarised as follows:

a) The larger the crack width, the greater the RM.

b) The greater the vehicle speed, the smaller the RM.

c) The larger the aggregate size, the smaller the RM.

d) The higher the elastic modulus of the concrete the smaller the RM for the same LTE.

e) The higher the elastic modulus of the subbase, the smaller the RM, also for the same LTE.

6.1.2 Dowel modelling

A thorough literature review was conducted to investigate existing methods for modelling steel dowel/concrete interaction at joints in jointed concrete. It was concluded that the main function of dowels is to prevent faulting, reduce pumping, and reduce corner breaks. From the literature review, as well as the theoretical dowel modelling, it is obvious that even relatively small gaps around the dowels has a significant effect on joint displacements, and the ability of the dowel to transfer shear load from the loaded to the unloaded slab (Davids et al, 1998a, 1998b). These gaps are already in existence at the time of construction over at least half the length of the dowel, because of de-bonding agents, or sleeves around the dowels. It is therefore just a matter of time before the other half of the dowel also develops a gap around it, and that the shear force transferred through the dowel reduces to such an extent that it approximates the shear force transferred across the joint through aggregate interlock only. This was plainly presented in Appendix D where the combined affect of aggregate interlock and dowel modelling with both an increase in crack width and an increase in the gap width around the dowel was investigated theoretically. In effect these facts imply that eventually the main function of dowels revert back to that which has been stated at the beginning of this paragraph, that of preventing faulting, reducing pumping, and reducing corner breaks. Dowel bars can therefore be expected to act as load transfer devices, but it should not be expected of a dowel bar to transfer shear forces across the joint, once dowel looseness has developed.

Research done by Hammons and Ioannides (1996) emphasised the fact that accurate theoretical equations for dowel modelling have been in place since the 1930's. It was pointed out that the so-called Friberg (1940) equations, based on the original Westergaard (1926) theory, are still applicable. The Friberg (1940) equations also form the basis of the dowel load transfer coefficient determined for the new mechanistic M10 design method (Strauss et al, 2001). It was therefore not deemed necessary to concentrate on dowel modelling experiments at this stage, but focus on the aspects involved with aggregate interlock modelling.

6.1.3 Field investigation

When addressing the first secondary objective stated in Chapter 1, field measurements of crack widths, LTE, and the RM at joints of four existing jointed concrete pavements in South Africa were obtained.

At the time of investigation, the ages of the four pavements were 32, 14, 23, and 13 years, respectively.

According to the reports from which the data was taken, the predicted remaining lives of each road section was 4, 14, 6, and 20 years, respectively. CncRisk analyses gave more pessimistic remaining life results, especially for Road Section 4. Road Section 4 had comparatively high RM measurements at the joints, which were not only due to the test load on the pavement, but also due to temperature effects, as well as the probability of voids beneath the concrete. This emphasised the importance of proper maintenance of concrete pavement joints. Properly sealed and maintained joints prevent the ingress of water and debris into the pavement structure, which in turn cause poor LTE or high RMs at joints relying on aggregate interlock.

The field data was also used to calibrate the laboratory results. The shift factor to adjust the laboratory RM versus LTE data to the field data was a function of the subgrade modulus (k), radius of relative stiffness (l) and the subbase stiffness ($E_{subbase}$). For the equation $LTE = e^{F*RM}$, the combination that gave the closest results for the shift factor (F) was:

$$F = l/(k*E_{subbase}) \tag{6.2}$$

In effect this calibration of the data has also shown that one of the main objectives of the particular test set-up used for the aggregate interlock experiments has been achieved. Through the specific test set-up, an attempt has been made to test the effects of aggregate interlock, and although the load transfer efficiencies were optimistic when compared to the field data, the range of RMs over which load transfer takes place through aggregate interlock has been established. This range varies from approximately 0 mm to 0,12 mm, especially for the smaller 19 mm coarse aggregate. Indications are however, that for larger 37,5 mm coarse aggregates this range extends past the values tested. At larger RMs the subbase influenced the results to a great extent, which is clearly shown by the RM of the smooth plastic joint. The main contribution of the plastic joint results in combination with the aggregate interlock results therefore, was that the same range of RM measurements as the field measurements was obtained. This therefore clearly indicated where the LTE measured in the field, relies mainly on the subbase stiffness, due to either crack widths larger than 2,5 mm, or an aggregate crack face that has been abraded under traffic movement to such an extent that it gives the same RM results as a smooth joint.

6.2 CONCLUSIONS

The main conclusions reached after interpretation of experimental results were as follows:

a) An increase in crack width caused an increase in deflection, a decrease in deflection LTE, and an increase in RM.

b) The larger 37,5 mm aggregate had lower deflections than the smaller 19 mm aggregate at the same crack widths during dynamic and static loading.

c) Beyond a crack width of 2,5 mm the data for the 19 mm coarse aggregate tended to remain constant, and it was therefore not considered necessary to test at crack widths greater than 2,5 mm. It was specifically stated in previous research studies (Davids et al, 1998b; Jensen, 2001) that at crack widths greater than 2,5 mm the stiffness of the subbase starts to play a role in levelling out the measured response of the slabs. However, this study has shown that the smoother the texture of the crack face, the sooner the system would rely on the support of the subbase to transfer stresses and strains from one slab to another. This study has indicated three such transition zones, namely: 1,5 mm for the smooth joint, 2,5 mm for the 19 mm aggregate interlock joint, and between 3,5 mm and 4,0 mm for the 37,5 mm aggregate interlock joint.

d) At small crack widths (< 0,5 mm) the bottom crack displacement measurements tended to be higher than the top crack displacement measurements. The slab tended to bend through with the top of the crack closing, and the bottom of the crack opening during loading. This was more evident during dynamic loading than during static loading, due to the effects of momentum.

e) At crack widths greater than 0,5 mm the top crack displacement became larger than the bottom crack displacement, indicating that the crack was being pushed open during loading. This demonstrated why large crack widths are so detrimental to pavement performance, as the opening up of the crack at the top during loading, makes it easier for debris and loose particles to be driven into the cracks, which in turn cause spalling of the concrete at the crack face. Once again the effect was greater during dynamic than static loading.

f) The deflection LTE was greater during dynamic than static loading in all instances. Larger sized coarse aggregates had greater deflection load transfer efficiencies than smaller sized coarse aggregates.

g) For the same coarse aggregate size concrete mixes, the LTE was larger where there was a continuous subbase support (rubber not cut through) than where there was a crack simulated into the subbase (top rubber layer cut through).

h) Due to the effects of momentum forces acting across the crack, the LTE under 40 kN static loading was higher than under 20 kN static loading.

i) Due to the effects of momentum acting across the joint, the LTE under dynamic loading of a bubble plastic joint on the non-continuous subbase remained remarkably high (92% at a crack width of 2,5 mm), compared to the gradual decrease in LTE with increasing crack width under static loading (18% at a crack width of 2,5 mm).

j) Although the deflections were in the same order of magnitude, the load transfer efficiencies achieved using South African crushed stone were significantly higher when compared to published results. The 19 mm dolomite aggregate rendered greater load transfer efficiencies than a 50 mm glacial gravel blend commonly used in the USA.

k) The joint shear stiffness (*AGG*) under dynamic loading was approximately 1,5 times that of the *AGG* under static loading on the continuous rubber subbase, and approximately 3 times higher on the discontinuous rubber subbase.

l) The range of shear stiffness per unit length of crack face that could typically be expected from South African aggregates (for crack widths of 0,1 mm to 2,5 mm) under static loading has been established.

During the experiments conducted for this research project, an attempt has been made to reach a better understanding of the intricacies involved in defining the mechanism of aggregate interlock. This mechanism can only be understood adequately if it is borne in mind that normal stress, shear stress, crack width, and shear displacement are all involved. On the other hand, concrete strength, aggregate size, and subbase support also influenced the results.

Tests on cracks subjected to earthquake loading Walraven (1981) showed that there is a considerable difference between the first and the subsequent loading cycles. Irreversible damage to the cement matrix takes place when the hard aggregate particles are pushed into this softer cement matrix. Any new cycle of loading leads to further damage of the crack faces, resulting into steadily increasing values of the shear displacement and the crack width at peak loading. In effect this was also proven during this study. The load applied to induce the crack in the less than 24-hour old concrete can be described as the first loading cycle, during which irreversible damage took place, in other words, during which the crack was formed. Subsequent loading and opening and closing of the crack caused further damage and the dislodging of fine particles that prevented the closing of the crack back to 0,1 mm once it has been pulled open.

Yet, despite this "damage" to the crack faces, the results obtained using the high quality crushed stone found in South Africa were superior to results obtained using USA aggregates. The common practice in South Africa of constructing jointed concrete pavements without dowels at the joints relying on aggregate interlock load transfer only has therefore been vindicated by this study.

The main contribution to the current state of knowledge was the development of a mechanistic equation quantifying the effect of aggregate interlock at a joint/crack in a concrete pavement. This equation has already been included and tested in the CncRisk software package, developed as part of the upgrading of the new mechanistic concrete pavement design manual for Southern Africa.

6.3 RECOMMENDATIONS

Further research is required to confirm up till which crack width aggregate interlock is still active for the larger 37,5 mm coarse aggregate, as the deflection results did not reach an asymptote at a crack width of 2,5 mm.

An aspect that has not been specifically addressed during the present study, was the effect of abrasion or aggregate wear out within the aggregate interlock joint, as little abrasion took place during

application of the 2 million dynamic load cycles at the initial crack width. As mentioned, this was partly due to the little relative vertical movement that could take place in the still "locked-up" state of the crack. Abrasion within the aggregate interlock joint should be established by applying up to 2 million dynamic loads across the crack at different crack widths, and measuring the deterioration in LTE.

The equation developed for the aggregate interlock factor, using data from this research study has already been included and tested in the CncRisk software package, as part of the upgrading of the new mechanistic concrete pavement design manual for Southern Africa, and can be used with confidence. The literature review on dowel modelling has also shown that the theory applied in the software does not need revision. Equation (6.1) does not include slab thickness as a variable, due to the fact that all the experimental slabs were 230 mm thick. It is logical that the shear stress developed at the crack face of a thin concrete slab will be less than the shear stress developed at the crack face of a thick concrete slab. Exactly how slab thickness forms part of the equation will have to be determined through follow-up testing. Another aspect that has been identified is that the erosion model used in the software needs revision. This can also be determined through further research projects.

6.3.1 Follow-up testing

The success of this study has laid the foundation for further testing involving dowel bars, as well as different subbase types to study the effect of erosion.

It is proposed that a test method similar to that used by Snyder (1989) be developed for testing dowel looseness in concrete. Instead of inserting the dowel bars into the concrete afterwards (as was done in the concrete repair study by Snyder (1989)), it should however be cast into the concrete from the start. The dowel should be instrumented with strain gauges on at least three positions inside the embedment length, as well as close to the edge of the concrete, in order to measure the bending moment on the dowel bar. The dowel should be subjected to cyclic loading with complete stress reversal at a frequency of 3 Hz. A method should be devised for measuring the movement in the dowel, and determine after how many load cycles dowel looseness started to develop, as well as the size of the gap created during loading. The method used by Snyder (1989) with a linear variable displacement transducer (LVDT) mounted on an aluminium bracket attached to the face of each specimen and connected to the load collar using a small threaded nylon rod, seems to have been quite successful. This device was used to measure electronically the movement of the load collar and dowel relative to the concrete. In this manner different dowel diameters, as well as specimens with different aggregate types, can be tested.

Erosion of the subbase can be determined by constructing various types of subbases inside a timber box. It is proposed that the same dimensions, namely 230 mm thick, 600 mm wide, and 1 800 mm long concrete beams be cast. The mould for the concrete can be fastened onto the timber, and the concrete

beam with crack inducer and flat bar can be cast on top of it as has been done in the study described in this document. The crack should be induced within 24 hours after casting the concrete. During testing, deflections should be measured with LVDT's on top of the concrete, and at the top and bottom of the subbase. The timber box containing the subbase should be constructed in such a manner that the section beneath the joint/crack in the concrete is visible/accessible from both sides with for example, removable panels. The concrete slab can then be subjected to dynamic loading, as was done during the initial stages of this study. The development of erosion as well as a reflection crack, if any, can then be monitored.

In a test set-up similar to the one used in the research done for this thesis, an eroded subbase can also be simulated by cutting away specific lengths of rubber beneath the leave slab. The effect of "erosion" on aggregate interlock LTE under static and dynamic loading can then be determined.